

# Blood vessel staining in the myocardium for 3D visualization down to the smallest capillaries

Bert Müller<sup>a,\*</sup>, Jens Fischer<sup>a,b</sup>, Ulrich Dietz<sup>c</sup>, Philipp J. Thurner<sup>a,d</sup>, Felix Beckmann<sup>e</sup>

<sup>a</sup> Computer Vision Laboratory, ETH Zürich, Gloriastrasse 35, Sternwartstr. 7, 8092 Zürich, Switzerland

<sup>b</sup> Medizinische Hochschule Hannover, Anna-von-Borries-Str. 1-7, 30625 Hannover, Germany

<sup>c</sup> Deutsche Klinik für Diagnostik, Aukammallee 33, 65191 Wiesbaden, Germany

<sup>d</sup> University of California, Santa Barbara, CA 93106, USA

<sup>e</sup> GKSS-Forschungszentrum, Max Planck Str. 1, 21502 Geesthacht, Germany

Available online 3 February 2006

## Abstract

Blood vessels formed after medical interventions such as radiofrequency treatment have to be visualized down to the capillary level with diameters of about 5  $\mu\text{m}$  to validate neo-vascularization. Synchrotron radiation-based micro-computed tomography (SR $\mu$ CT) provides the necessary spatial resolution. Since both the vessels and the surrounding tissue mainly consist of water the difference in absorption is extremely weak. Therefore, it is necessary to search for appropriate contrast agents and to develop suitable staining protocols, which finally allow segmenting the vessel tree. Among the contrast agents used in medicine lyophilic salts with a mean particle diameter of 1.5  $\mu\text{m}$  such as CaSO<sub>4</sub>, SrSO<sub>4</sub> and BaSO<sub>4</sub> are most appropriate to stain the vessels. The combination of these salts with a commercially available embedding kit (JB-4, Polysciences Inc.) allows tissue fixation and long-term storage in solid state. Intensity-based segmentation algorithms enable the vessel tree extraction in selected parts of the stained myocardium using the SR $\mu$ CT data.

© 2005 Elsevier B.V. All rights reserved.

PACS: 47.63.Jd; 47.63.Cb; 81.70.Tx; 87.59.Fm; 87.57.–s; 41.60.Ap

Keywords: Imaging techniques; Computerized tomography; Myocardium; Blood vessels; Staining; Biomedical engineering

## 1. Introduction

Treatments of cardiovascular diseases belong to medical interventions of eminent socioeconomic impact. For almost one century, numerous efforts have been made to improve the blood supply in chronically ischemic myocardium of patients, who have occlusive coronary artery disease unsuitable for revascularization of the native coronary arteries [1,2]. There exist three routes for the alternative blood supply, i.e. from epicardial sites, transmural from the border zone (collaterals) and from the endocardium [3–5]. These procedures are aimed at ini-

tiating iatrogenic vasculogenesis. The direct supply of the myocardium with blood from the left ventricle certainly is the major blood supply route in the reptilian heart, which relies on the perfusion of the well-developed system of sinusoidal channels [6–8]. It was shown that tissue adjacent to myocardial channels, acutely created by laser direct myocardial revascularization (DMR), can be perfused by blood from the left ventricle [7,9,10]. Therefore, the blood entering the myocardium by patent channels is likely drained by the sinusoidal channel system [11,12]. Furthermore, the perfusion of the sinusoidal system can take over nutritive functions [13,14]. Consequently, such a mechanism can support re-establishing the supply of the myocardium with the sufficient amount of blood.

For the two treatments, needle acupuncture and laser-induced intra- or transmural channels, the blood flow

\* Corresponding author. Tel.: +41 1 6336190; fax: +41 1 6321199.  
E-mail address: [bmuller@vision.ee.ethz.ch](mailto:bmuller@vision.ee.ethz.ch) (B. Müller).

in the myocardium could be instituted. Most of the channels, however, become occluded by collapsing and thrombosis after needle acupuncture or a strong fibrotic scar formed after laser application. Searching for a promising alternative, we introduced the concept of myocardial thermo-modulation using high-frequency (HF) energy deposition at the frequency of about 500 kHz to induce connective heating of the tissue surrounding mechanically created intra-myocardial channels. In an earlier study, we investigated the short-term effects of this treatment in an animal study using rabbit hearts. We found that the channels created with the 0.7 mm probe persisted for at least 4 h with only a very few being occluded by thrombus [15]. In order to investigate the long-term effects, we have chosen pig hearts, which better resemble the situation in the human body. We demonstrated the feasibility of a transluminal approach for applying temperature-regulated HF-ablation to form intra-myocardial channels. Using classical histology, we found a high rate of patent channels in the acute setting, a finding comparable to the results of our former work with the rabbit hearts. In keeping with observations in the rabbit hearts, numerous open connections to myocardial sinusoids were documented. This experimental finding is associated with the tissue welding, achieved by locally applied heat in the temperature range between 60 and 140 °C [16,17]. Since perfusion studies were not performed, the physiological relevance of these connections is not proven yet. The formation of a significant number of connections, however, is expected to institute flow through the channels and, hereby, to reduce the probability of the acute thrombotic occlusion. In our preliminary experiments, most of the channels were only partially obstructed by thrombus, which is interpreted as the result of channel perfusion preventing blood coagulation. In the acute setting, the thermally damaged myocardium exhibited no structural changes shown by histological sectioning. We confirmed the high reproducibility of dimensions of the thermally damaged zones using the temperature-controlled HF-energy application mode. The dimensions of the damaged zones are comparable to that found in a previous investigation with identical energy delivery [15].

The replacement of irreversibly damaged myocardium seems to proceed slower than in the comparable analysis using laser transmural myocardial revascularization (TMR), in which the complete removal of myocardium and the conversion to the scar tissue was observed within one month [18–20]. The observation of the dense meshwork of erythrocyte traces running through the central portion of the degenerating myocardium three weeks after HF application, percutaneous myocardial revascularization (PMR) indicates that the process of neo-vessel formation is more pronounced after HF-energy delivery than after laser treatment. Unfortunately, for the laser DMR the histological results were not described. After nine weeks, the scarring was completed as indicated by large amount of collagen fibres in the scar tissue and the significant reduction of fibroblast content to less than 5% of the scar area.

The scarring process is accompanied by the disappearance of measurable channel lumen in the majority of preparations, although there were some clefts in the centre of the fibrotic zones containing fresh red blood cells. In one heart, the left ventricle was filled with gelatine applying the pressure of 10,666 Pa (80 mmHg). We could demonstrate that the newly formed vessels within the fibrotic zones were filled with gelatine verifying the existence of functional connections with the left ventricular cavity. Since the coronary circulation was carefully ligated and no gelatine observed in remote areas of the myocardium, we are confident that the newly formed vessels accomplish functional communications with the left ventricular cavity. Because gelatine was also found within sinusoidal vessels adjacent to the fibrotic areas, we speculate that a ventriculo-sinusoidal circulation was achieved [21].

In order to quantify the success of the intervention, however, the 3D morphology of the blood vessel system within the region of interest has to be precisely determined. Whereas classical histology is a well-established, versatile tool for 2D analysis of different kinds of tissue, the 3D characterisation via serial sectioning is very tedious and time-consuming. Important parameters in the case neo-vascularization such as the number of connections in the newly formed capillary tree are thus not readily accessible using histology. Therefore, micro-computed tomography ( $\mu$ CT) has been used as complementary technique to visualize the vessels in the myocardium [22]. These images, however, only show voxel gradient shading and maximum intensity projection representations with the voxel size of 30  $\mu$ m. Consequently, the smallest blood vessels are not uncovered, and the quantitative characterisation of the neo-vascularization is questionable. Using synchrotron radiation (SR $\mu$ CT), the isotropic spatial resolution in the three orthogonal directions is further improved and the application of the monochromatic beam allows the quantitative analysis of bony [23] and soft [24,25] tissues. The photon energy at the synchrotron radiation sources can be tuned to sample size and average absorption [26]. Hence, SR $\mu$ CT offers to resolve the vessels down to the smallest capillaries in specimen of several millimetres, to uncover the connections of myocardial capillaries and larger vessels to the channels created acutely and to the capillaries formed during scar formation after HF myocardial ablation. In addition, the extent of the myocardial vessels that can be filled up from the left ventricular cavity via the channels or capillaries formed by the HF myocardial ablation could be quantified for the entire myocardium sample. Since SR $\mu$ CT is non-destructive, the specimen can be subjected to histology after the measurements to gain complementary information. The SR $\mu$ CT-data might even be exploit to identify regions of interest for the histological characterisation.

One of the most important problems applying SR $\mu$ CT to biological systems is the development and verification of appropriate sample preparation. On the one hand, the sample should be in a state as close as possible to the

in vivo situation to reduce preparation artefacts whenever possible. Much simpler, on the other hand, is the use of a well-established embedding technique known from histology to form samples to be stored until beamtime is available. Subsequently, the destructive histological studies can be carried out.

Since biological tissue consists mainly of water, the system of blood vessels in the myocardium cannot be distinguished per se in the absorption contrast mode [27]. Consequently, the search for promising staining techniques is highly desirable. The open question is, how a sufficient amount of higher or lower absorbing agents can be injected into the vessels without significant migration into the surrounding tissue. First of all, suitable staining materials have to be identified. In this study we have injected different materials well known from other staining purposes in medicine containing the elements I, Au, Gd, Os, Ba, Sr or Ca. The injection of particles smaller than the thinnest capillaries, which cannot migrate

through the walls of the vessels and are insoluble in the wet environment, is expected to be the basis of the desired staining procedure.

## 2. Experimental

The study is based on the left ventricle of porcine heart tissue (Deutsche Landrasse). The weight of the animals varied between 92 and 128 kg resulting in hearts of about 300 g. For sample fixation and conservation the commercially available embedding kit JB-4 (Polysciences Inc., Warrington, PA, USA) was used. The kit was applied as recommended by the producer. To avoid the formation of bubbles, however, the monomer was cold down to 4 °C and degassed at the pressure of 20,000 Pa (200 mbar).

For the injection of the contrast agent, the higher absorbing material was mixed with the monomer solution of the embedding kit using the magnet mixer at relatively low rotation speed.

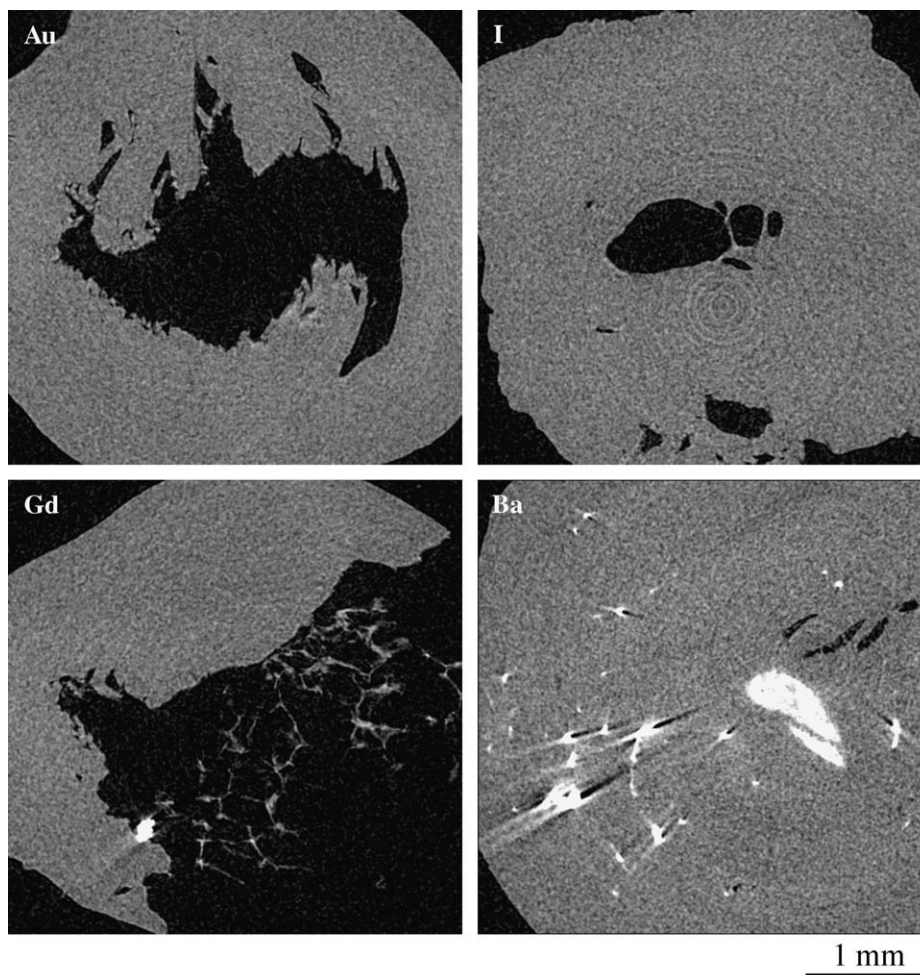


Fig. 1. The availability of synchrotron radiation facilities is much more restricted than the use of desktop  $\mu$ CT-systems. Therefore, we used a desktop  $\mu$ CT-system ( $\mu$ CT 40 Scanco Medical AG, Bassersdorf, Switzerland) to identify the most promising staining materials for the blood vessels in the myocardium. Selected  $\mu$ CT-slices of gold, iodine, gadolinium and barium stains demonstrate that the use of gold and iodine was not successful, since no vessel comes to light. The gadolinium stain is seen to be located exclusively in a very few larger vessels and seems to be less suitable for the staining of the capillaries. The barium salt, however, gives rise to the network of very strong absorbing areas representing vessels of different size. Note that the absorption of the tissue is almost identical for the differently stained myocardium samples.

One milliliter of goldconjugate as used in previous studies [24,25] was mixed with 5 ml monomer solution. Just before the injection 0.2 ml of the catalyst (solution B of the embedding kit, benzoyl peroxide) was added. This mixture was injected into several arteries of the myocardium. For this study the injection took place 15 min after the pig was sacrificed, avoiding significant autolysis. During the injection the resistance steadily increases because the viscosity of the mixture rises. Visually, in the larger vessels, one could observe the colour change of the tissue from red to white related to the entering and the polymerization of the mixture. Therefore, the vessels were labelled and the region of interest could be selected. Tissue samples with the diameter of about 4 mm and the length of around 8 mm were extracted with the scalpel and, subsequently, put into 1.5 ml Eppendorf-tubes. Then, the monomer solution was added and exchanged after 2 h. After additional 11 h, the catalyst was added. Three hours later the sample preparation was finalized. The myocardium tissue was conserved in solid state.

Iodine is also a common contrast agent in medicine, for example to make visible the vessel system during angiography. It is directly injected into the vessel system and provides strong contrast for the vessels with respect to the surrounding tissue. For the present study, 0.25 ml iodine were mixed with 5 ml of the monomer solution.

Another element common in use as contrast agent is gadolinium. This element in combination with diethylenetriaminepentaacetic acid, gadolinium(III) dihydrogen salt hydrate (DTPA) has its special application in magnet resonance imaging due to its paramagnetic properties. Twenty-one milligrams of the solid powder gadolinium–DTPA (97% Aldrich Chemical Company Inc.) were mixed with 3 ml of the monomer solution.

Osmium tetroxide ( $\text{OsO}_4$ ) is used as contrast agent and to fixate organic matter. Well known from electron microscopy it was also successfully applied to stain cell cultures for SR $\mu$ CT [24,28]. Since the osmium compound is mainly bound to the lipids of the cell membrane, one might expect to mark the tissue and not the vessels. Consequently, the vessels should be uncovered because of lower absorption with respect to the surrounding tissue. To stain the myocardium by  $\text{OsO}_4$ , the piece of interest with the diameter of about 4 mm and the length of about 5 mm was put into a dish before the  $\text{OsO}_4$  was added. After 4 h the rest of the chemical was neutralized and prepared as the gold-stained myocardium.

Lyophilic salts such as  $\text{CaSO}_4$ ,  $\text{SrSO}_4$  and especially  $\text{BaSO}_4$  are often used as contrast agents in clinical environment to visualize the stomach and more often the bowel by means of computed tomography with X-rays. These agents are strongly hydrophobic. Thus, they do not migrate through the wall of stomach and bowel into the body. They are inert and stay only in the region of interest for a well-defined period of time. For the experiments, we have chosen powdered salts with the mean particle diameter of 1.5  $\mu\text{m}$ , which is well below the diameter of the smallest

blood vessels. Four hundred and fifty milligrams of  $\text{BaSO}_4$  (Art. 11845, Fluka Chemie GmbH, Switzerland),  $\text{SrSO}_4$  (Art. 85898, Fluka Chemie GmbH, Switzerland) and  $\text{CaSO}_4$  (Art. 21244, Fluka Chemie GmbH, Switzerland), respectively, are mixed with 3 ml of the monomer solution of the embedding kit. The salts were injected into the following heart vessels: Margo ventricularis sinister ( $\text{BaSO}_4$ ), Ventriculus sinister ( $\text{SrSO}_4$  and  $\text{CaSO}_4$ ) and Ventriculus dexter ( $\text{CaSO}_4$ ).

In order to get a first overview of the differently stained samples, conventional micro-computed tomography ( $\mu\text{CT}$  40, Scanco Medical AG, Bassersdorf, Switzerland) was used.

The SR $\mu$ CT measurements were carried out at the beamlines BW2 and W2 (HASYLAB at DESY, Hamburg, Germany), i.e. a synchrotron radiation source of second generation [29], and the materials science beamline 4S (SLS at PSI, Villigen, Switzerland), a synchrotron radiation source of third generation, with the standard set-up for absorption contrast [30]. The different parameters used for the tomographic imaging are given in the text below and the figure captions.

The SR $\mu$ CT tomograms from the beamline BW2 (HASYLAB at DESY) lead to histograms of the local absorption coefficients that have exactly the Gaussian shape [31]. Therefore, it is rather simple to determine the intensity-based threshold for the segmentation of the appropriately stained vessels. The histograms extracted from the different tomograms were fitted with Gaussians (pro Fit 5.5.3, Quantumsoft, Zurich, Switzerland) using the Levenberg–Marquardt algorithm [32]. The thresholds

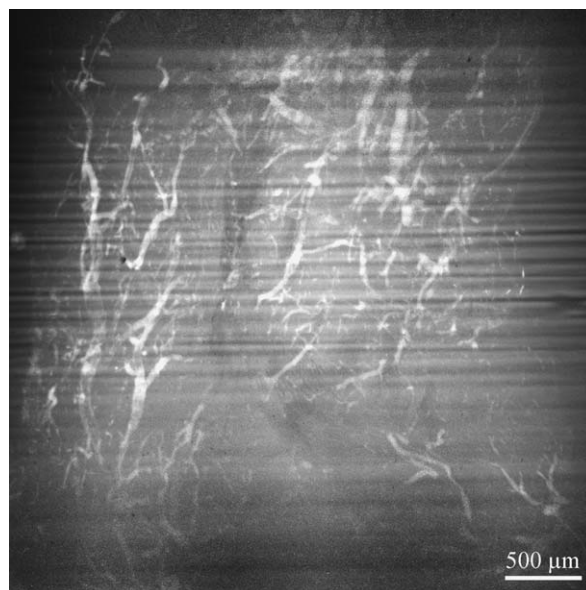


Fig. 2. The projection of the  $\text{BaSO}_4$ -stained sample very clearly shows the network of blood vessels in the myocardium. The image was acquired at the materials science beamline 4S (SLS, Villigen, Switzerland) using the photon energy of 10 keV and the illumination time of 2.6 s. Note that the instability of the synchrotron X-ray beam resulted in intensity modulations, although the image is background corrected.

for the different phases were set at the intersections of the Gaussians for the adjacent phases. Commercial software was applied for the 3D visualization of the vessel network (VG Studio Max, Volume Graphics, Heidelberg, Germany).

### 3. Results

To identify the most promising staining materials, conventional  $\mu$ CT was used. The tomograms verify that the sulphates are the most appropriate materials to stain the smaller vessels as can be seen in Fig. 1. Alternatively, radiography of the differently stained samples at the beamline 4S was performed, substantiating the conventional results.

The typical projection of the  $\text{BaSO}_4$ -stained sample represented in Fig. 2 exhibits the complex network of stained blood vessels with diameters between tenths of a millimetre and less than  $10\ \mu\text{m}$ .

Below the photon energy of 20 keV the intensity at the beamline W2 drops down. From the radiographic imaging, however, the optimal photon energy to visualize the matrix (embedded myocardium) of the samples with the diameter of 4 mm, related to the total projected absorption that approximately corresponds to two [26], is between 10 and 13 keV. The optimized photon energies for the stained areas are usually higher and depend on the nature of the selected stain [24]. Nevertheless, the photon energy of 20 keV is above the optimal energy for the embedded and

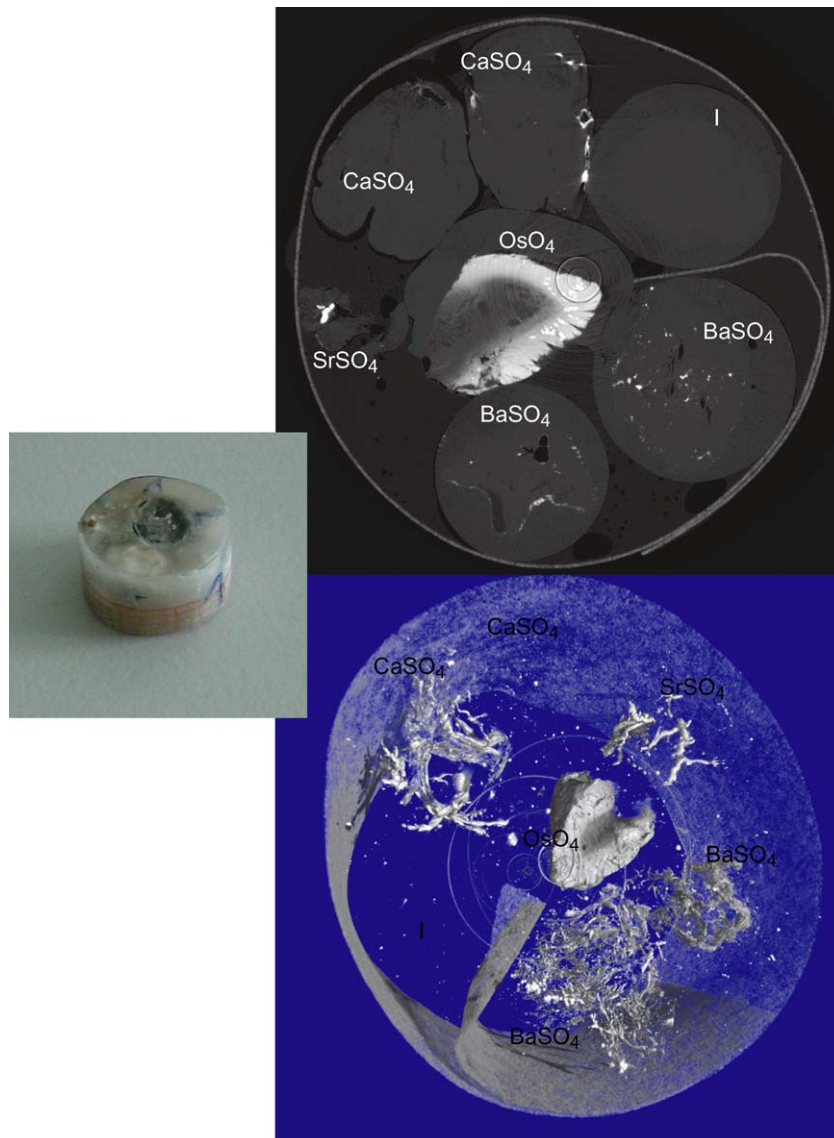


Fig. 3. The individual vessel-stained myocardium specimens each about 4 mm in diameter are combined to form a sample with a diameter of 12 mm in order to realize a reasonable total projected absorption of the sample at the lowest possible photon energy at the beamline W2 (HASYLAB at DESY, Hamburg, Germany) of 20 keV and to have the direct comparison between the staining materials for the blood vessels. Besides the photograph, one typical slice of the tomogram and the 3D representation based on the tomogram are shown. The different stains are indicated. As marker we incorporated a piece of paper surrounding the sample that exhibits a higher absorption than the embedding material.

stained myocardium specimens. Therefore, we combined the specimens to increase the total absorption of the entire sample, as illustrated in Fig. 3 by the photograph, the slice and the 3D representation. The simultaneous measurement allows the precise and direct comparison of the differently stained specimens. The disadvantage of this approach is the reduced spatial resolution. In order to partly compensate the reduction of the spatial resolution, the rotation axis was asymmetrically placed, and the sample rotated by  $360^\circ$ . Therefore, only half of the sample was recorded in the parallel projection and suitably combined before

reconstruction. Such a procedure allows improving the spatial resolution by a factor of 2, resulting in the voxel length of  $5\ \mu\text{m}$ .

To determine the threshold for the vessel segmentation, the histograms of the absorption values within the region of interest were analyzed. As in previous studies, the histograms of the absorption values exhibit Gaussian distributions for each component [23,28,31]. The peaks are separated. Consequently, the crossing point of the Gaussians is the appropriate choice for the threshold. The experimental data and the related fits selected from

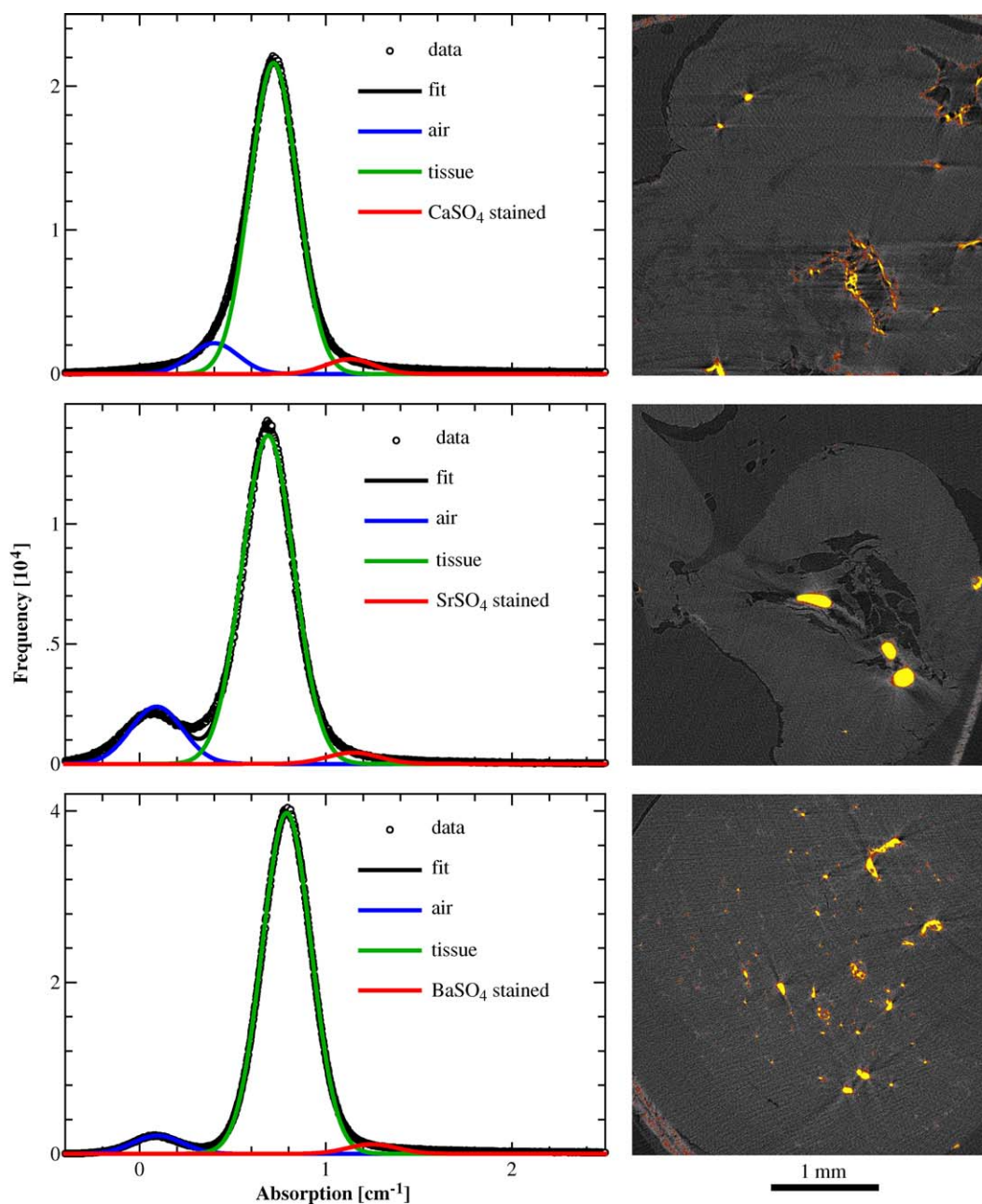


Fig. 4. The histograms of the absorption values of the regions of interest from the samples with different sulphate staining indicate that the three salts containing Ca, Sr and Ba are well suited for the visualization of the blood vessels in the myocardium. On the right hand side, the related typical tomographic slices each with a size of  $(3.3\ \text{mm})^2$  are given. Here both the tissue (grey-coloured) and the stained vessels (yellow) are visible. (For interpretation of the references in colour in this figure legend, the reader is referred to the web version of this article.)

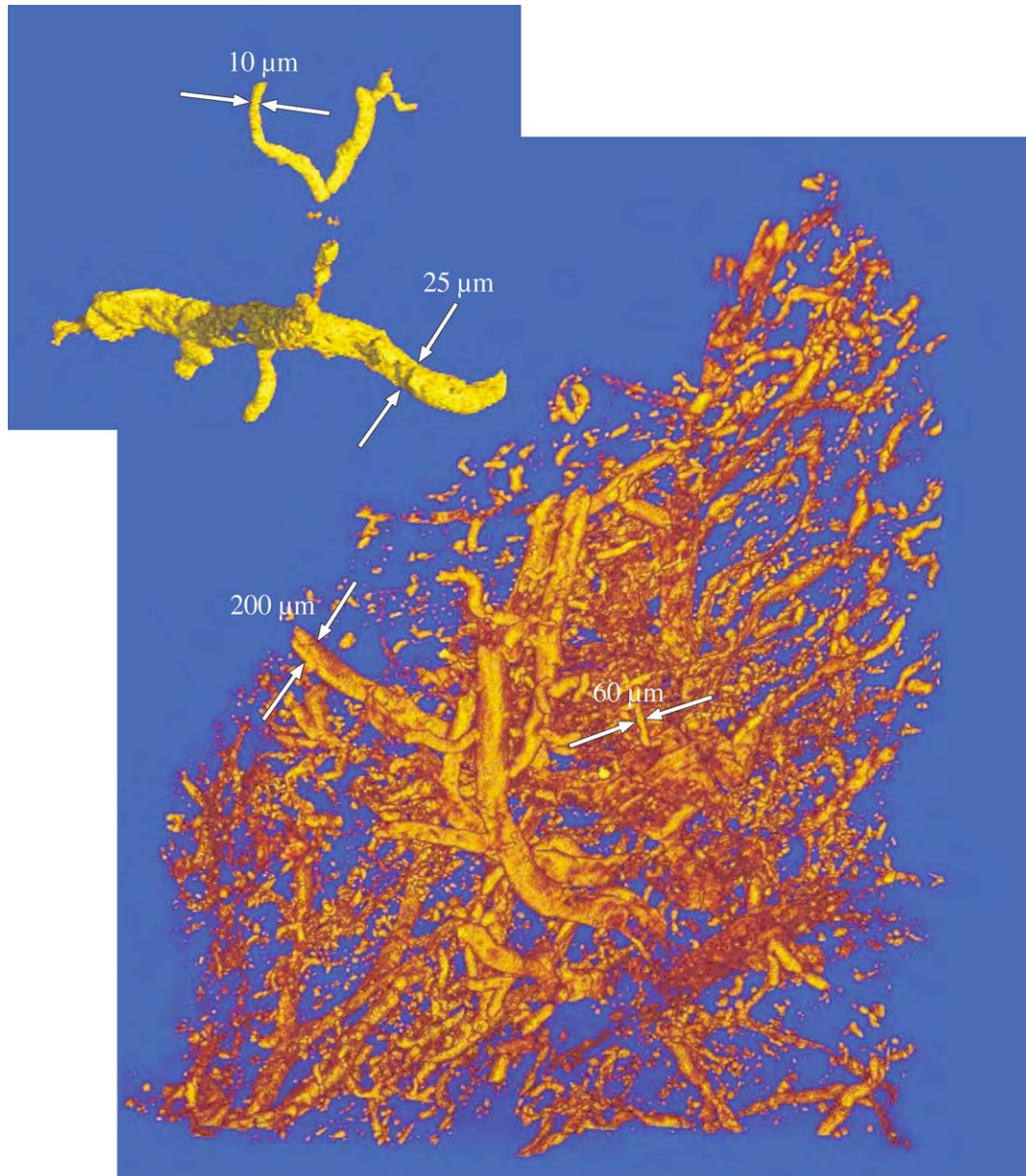


Fig. 5.  $\text{BaSO}_4$  staining allows the visualization of the complex vessel tree in the myocardium. The vessels represented have diameters between a few tenths of millimetre and  $10\ \mu\text{m}$ . Note that several vessels appear to be disconnected, presumably the result of the inhomogeneous stain distribution.

the tomogram for the three different sulphate stains containing Ca, Sr and Ba, respectively, are shown in Fig. 4 together with typical tomographic slices.

In Fig. 5 a 3D visualization of the  $\text{BaSO}_4$ -stained sample is presented. Here, the intensity-based segmentation of the 3D vessel tree in the myocardium is feasible: vessels with diameters between tenths of a millimetre and less than  $10\ \mu\text{m}$  can be clearly identified. The thinnest yellow-coloured vessels shown in the inset represent capillaries with the diameter of 2 voxel lengths ( $10\ \mu\text{m}$ ).

#### 4. Discussion and conclusion

The used embedding kit JB-4 is the very promising alternative to the present, time-consuming infiltration and

exchange steps for tissue conservation and fixation. To avoid bubble formation resulting from the exothermic polymerization reactions and the remaining gases in the monomer solution, the solution A should be degassed and kept below  $10\ ^\circ\text{C}$  before and during polymerization.

The sample preparation procedure is much simpler than the casting-like staining and paraffin embedding performed by Kwon et al. [22].

Staining materials mixed with the embedding kit, which can penetrate the walls of the blood vessels, are inappropriate to stain the capillaries, because the stain concentration differences between vessels and surrounding tissues are too low.

Sulphate particles of micrometer size form a suspension when mixed with the monomer solution of the embedding

kit. During injection into the larger blood vessel the polymer solution transports the stain into the capillaries. The relatively large, insoluble particles cannot penetrate the wall and, therefore, stay within the vessels as shown by radiography and  $\mu$ CT. The presented tomograms show, however, that especially the vessels with diameters of some 10  $\mu$ m often appear to be disconnected. This phenomenon is attributed to the inhomogeneous stain distribution resulting from sedimentation processes of particles with different sizes and from local viscosity changes during polymerization. The optimization of particle density, particle size, particle size distribution and viscosity of the injected suspension, which was not part of the presented study, will presumably improve the staining efficiency. The viscosity, mainly given by the polymer, should be, on the one hand, low enough to allow entering the capillaries. Low viscosity, on the other hand, enhances the sedimentation process. Because the sedimentation velocity depends on the square of the particle diameter, the choice of particle size and size distribution is also crucial for optimization. The influence of the volume density difference between  $\text{CaSO}_4$  (2.96  $\text{g/cm}^3$ ),  $\text{SrSO}_4$  (3.96  $\text{g/cm}^3$ ) and  $\text{BaSO}_4$  (4.25  $\text{g/cm}^3$ ) on the one hand and the monomer solution (1.04  $\text{g/cm}^3$ ) on the other hand is of minor importance.

The identification of suitable staining materials and the successful development of the protocol to stain the blood vessels down to the thinnest capillaries and their non-destructive visualization by SR $\mu$ CT is a crucial step to verify neo-vascularization after medical treatments even in a quantitative manner.

### Acknowledgements

The authors thank the team at the veterinary faculty of the Zurich University, especially H. Augsburger, E. Bürgi and U. Müller for providing the fresh porcine hearts. The support of M. Stampanoni (SLS Villigen, Switzerland) at the materials science beamline and of the bioelectronics group, ETH Zürich for  $\mu$ CT imaging is gratefully acknowledged. The project was partially funded by Medtronic, Maastricht, Netherlands, by the Swiss National Science Foundation (Grant No. 2153-057127.99), by DESY, Hamburg, Germany (proposal I-02-068) and by SLS, Villigen, Switzerland (proposal 20030152).

### References

- [1] R. Moosdorf, F.C. Schoebel, W. Hort, Z. Kardiol. 86 (1997) 149.
- [2] R. Kornowski, M.K. Hong, M.B. Leon, Am. J. Cardiol. 81 (1998) 44e.

- [3] A.M. Vineberg, K.S. Baichwal, J. Myers, Surgery 57 (1964) 836.
- [4] W.N. O'Connor, J.B. Cash, C.M. Cottrill, G.L. Johnson, J.A. Noonan, Circulation 66 (1982) 1078.
- [5] A. Carpentier, J.C. Chachques, P. Grandjean (Eds.), Cardiac Bioassist, Futura Publishing Co., Inc., Armonk, NY, USA, 1997, p. 247.
- [6] J.T. Wearn, S.R. Mettier, T.G. Klumpp, I.J. Zschiesche, Am. Heart J. 9 (1933) 143.
- [7] D. Burkhoff, R. Fulton, K. Wharton, M.E. Billingham, R. Robbins, J. Thorac. Cardiovasc. Surg. 114 (1997) 497.
- [8] T. Kohmoto, M. Argenziano, N. Yamamoto, K.A. Vliet, A.G. Gu, C.M. Derosa, Circulation 95 (1997) 1585.
- [9] M. White, J.E. Hershey, Ann. Thorac. Surg. 6 (1968) 557.
- [10] P. Walter, H. Hundeshagen, H.G. Borst, Eur. Surg. Res. 3 (1971) 130.
- [11] J.T. Wearn, J. Exp. Med. 47 (1928) 293.
- [12] R.J. Tomanek, Cardiovasc. Res. 31 (1996) E46.
- [13] B.H. Oh, M. Volpini, M. Kambayashi, K. Murata, H.A. Rockman, G.S. Kassab, Circulation 86 (1992) 1265.
- [14] R.N. Gates, H. Laks, D.C. Drinkwater, J.M. Pearl, A.M. Zaragoza, W. Lewis, T.J. Sorensen, E.M. Kaczer, P.A. Chang, Ann. Thorac. Surg. 56 (1993) 410.
- [15] U. Dietz, M. Otto, M. Buerke, O. Eick, R. El Odhi, A. Förderer, Cardiology 93 (2000) 234.
- [16] R.D. Jenkins, I.N. Sinclair, R. Anand, A.G.J. Kalil, F.J. Schoen, J.R. Spears, Lasers Surg. Med. 8 (1988) 30.
- [17] G.E. Kopchok, R.A. White, G.H. White, R. Fujitani, J. Vlasak, L. Dykhovskiy, Lasers Surg. Med. 8 (1988) 584.
- [18] K.J. Fleischer, P.J. Goldschmidt Clermont, J.D. Fonger, G.M. Hutchins, R.H. Hruban, W.A. Baumgartner, Ann. Thorac. Surg. 62 (1996) 1051.
- [19] N. Gassler, H.O. Wintzer, H.M. Stubbe, A. Wullbrand, U. Helmchen, Circulation 95 (1997) 371.
- [20] T. Kohmoto, C.M. DeRosa, N. Yamamoto, P.E. Fisher, P. Failey, C.R. Smith, Ann. Thorac. Surg. 65 (1998) 1360.
- [21] U. Dietz, G. Horstick, T. Manke, M. Otto, O. Eick, C.J. Kirkpatrick, Cardiology 99 (2003) 32.
- [22] H.M. Kwon, B.K. Hong, G.J. Jang, D.S. Kim, E.Y. Choi, I.J. Kim, C.J. McKenna, E.L. Ritman, R.S. Schwartz, J. Korean Med. Sci. 14 (1999) 602.
- [23] R. Bernhardt, D. Scharnweber, B. Müller, P. Thurner, H. Schliephake, P. Wyss, F. Beckmann, J. Goebbels, H. Worch, Eur. Cells Mater. 7 (2004) 42.
- [24] P. Thurner, B. Müller, F. Beckmann, T. Weitkamp, C. Rau, R. Müller, J.A. Hubbell, U. Sennhauser, Nucl. Instr. and Meth. B 200 (2003) 397.
- [25] P. Thurner, B. Müller, U. Sennhauser, J. Hubbell, R. Müller, J. Phys.: Condens. Matter 16 (2004) S3499.
- [26] L. Grodzins, Nucl. Instr. and Meth. 206 (1983) 541.
- [27] J. Fischer, Mikrotomographie mit Synchrotronstrahlung, Gefäßdarstellung an biologischen Geweben, Fachhochschule Münster, 2003.
- [28] P. Thurner, F. Beckmann, B. Müller, Nucl. Instr. and Meth. B 225 (2004) 599.
- [29] F. Beckmann, Proc. SPIE 4503 (2002) 34.
- [30] M. Stampanoni, P. Wyss, R. Abela, G. Borchert, D. Vermeulen, P. Rügsegger, Proc. SPIE 4503 (2002) 178.
- [31] B. Müller, F. Beckmann, M. Huser, F. Maspero, G. Szekely, K. Ruffieux, P. Thurner, E. Wintermantel, Biomol. Eng. 19 (2002) 73.
- [32] D.W. Marquardt, J. Soc. Ind. Appl. Math. 11 (1969) 431.